Journal of Robotics and Control (JRC)
Volume 5, Issue 3, 2024
ISSN: 2715-5072, DOI: 10.18196/jrc.v5i3.21347

Improved Droop Control Based on Modified Osprey Optimization Algorithm in DC Microgrid

Widi Aribowo [1], Heri Suryoatmojo [2*], Feby Agung Pamuji [3]
[1, 2, 3]Department of Electrical Engineering, Institut Teknologi Sepuluh Nopember, Surabaya 60111, Indonesia
[1] Department of Electrical Engineering, Universitas Negeri Surabaya, Surabaya, Indonesia
Email: [1] 7022212006@mhs.its.ac.id, [2] suryomgt@ee.its.ac.id, [3] feby@ee.its.ac.id
*Corresponding Author

***Abstract*—In this research, a modified Osprey optimization algorithm (MOOA) is presented to optimize droop control parameters. MOOA is a modification of the Osprey optimization algorithm by adding levy flight which has the advantage of exploiting a wider space and being adaptive to environmental changes. This research also modifies droop control, Proportional Integral Derivative (PID) is applied to secondary control. PID has flexibility in responding to changes in system conditions and fast response in dealing with system changes. The PID parameters are optimized using MOOA and are called MOOA-PID. The MOOA method is validated using 23 CEC2017 benchmarks-function and performance on DC microgrid systems. This research uses the latest algorithms as a comparison, namely One-to-One Based Optimizer (OOBO), Preschool Educational Optimization Algorithm (PEOA), and the red-tailed hawk (RTH) algorithm in testing 23 CEC2017 benchmark functions. From the simulation of the 23 CEC2017 benchmark function, it is known that the MOOA method has better capabilities. MOOA has advantages in 15 out of 23 benchmark functions. In DC microgrid system testing, MOOA-PID is compared with the Proportional Integral (PI) method which is optimized with MOOA and is called MOOA-PI. Testing on the microgrid is aimed at determining the performance of the transient response of power, voltage and current in the system. Tests on DC microgrid systems found that the application of MOOA-PID in secondary control had better capabilities than MOOA-PI. The average value of voltage overshoot from MOOA-PID is 9.828% better than MOOA-PI. The average ITSE MOOA-PID score is 22.3% better than MOOA-PI.**

Keywords—Droop Control; Secondary Control; DC Microgrid; Metaheuristic; Optimization.

I. INTRODUCTION

Increased demand for electrical energy can be caused by various factors, and the primary causes may vary depending on the geographic, economic, social, and technological. Some common causes that can cause an increase in demand for electrical energy include economic growth, urbanization, increase in population, technological development, climate change and energy policy [1]–[5].

Geographical factors have a significant influence on the increasing demand for electrical energy. This is influenced by population distribution, infrastructure development, climate conditions, accessibility of energy sources, industrial development, and availability of renewable energy sources [6]. Several economic aspects that influence the demand for electrical energy include: economic growth, urbanization and urban development, industrial and business development, energy availability and costs, income levels and lifestyles, service sector growth and public service provision [7]. Several societal factors, such as changes in consumption patterns, urbanization, population growth, demographic shifts, lifestyle changes, and social welfare needs influence the demand for electrical energy [8], [9]. The growing need for electrical energy is mostly due to technological considerations. The following technological aspects have an impact on the demand for electrical energy: growing internet and information technology, electric vehicles and electric-powered transportation, smart grids and smart electric networks, internet of things (IOT) and connected devices, increasing use of electronic devices [10].

It is important to note that the combination of these factors often results in an increase in electrical energy demand in a region. Solutions to overcome these challenges involve a combination of energy efficiency, use of renewable energy sources, and development of sustainable energy infrastructure [11]–[13].

The use of renewable energy sources continues to grow throughout the world along with increasing awareness of the issues of climate change and energy sustainability. Some renewable energy sources that are generally used today include solar energy, wind energy, water energy, biomass, geothermal energy, wave, and tidal energy. The increased use of renewable energy sources is driven by several factors, including Environmental awareness, Technological Innovation, and Regulations and Policies [14]–[17]. Although the use of renewable energy continues to grow, there are still challenges such as the sustainability of energy storage and integration into the electricity grid [18]–[23]. Overcoming challenges related to renewable energy requires a holistic and integrated approach involving various aspects, from technology and infrastructure to policy and public awareness. several solutions that can help overcome some of the challenges in adopting and integrating renewable energy: technological innovation, energy infrastructure and storage, policy and regulation, public education and awareness, collaboration and partnerships, and integrated and sustainable approaches. Combining these solutions in a context that suits local needs and challenges will enable broader and more sustainable adoption and integration of renewable energy [24], [25].

A microgrid is a local energy distribution system consisting of renewable energy resources, energy storage systems, and electrical loads that are connected and operate

independently or can operate connected to the main electricity grid [26]–[31]. Microgrids are designed to provide electrical energy to specific areas or communities in a more efficient, sustainable and decentralized manner [32]–[37]. Some of the main characteristics of microgrids include renewable energy sources, energy storage systems, independent operation capability, centralized energy management, decentralization, automatic monitoring, and control. Microgrids can be deployed in a variety of locations, including urban, rural, and remote areas, and at various scales, from residential neighborhoods to industrial areas or university campuses. The existence of microgrids helps increase the efficiency, sustainability, and resilience of energy systems [38]–[41]. Each type of microgrid has certain advantages and disadvantages depending on its specific needs and operational context [42]–[47]. The use of a particular type of microgrid depends on the implementation objectives and the characteristics of the environment in which the microgrid is operated [48].

Microgrids can use alternating current (AC) or direct current (DC) depending on the specific needs and design of the microgrid. The choice between an AC or DC microgrid will depend on a variety of factors, including load characteristics, available resources, existing infrastructure, and the purpose of the system. Each type of microgrid has advantages and disadvantages, and their application must be carefully considered according to the specific needs of the project or application [49]–[51]. Alternating current (AC) microgrids have several advantages in many situations. Here are some of the advantages of ac microgrids: main power grid compatibility, efficient energy distribution, mature technology, voltage flexibility, easy to convert voltage, support for various loads, and renewable resources. Although AC microgrids have several advantages, as explained previously, there are several disadvantages that need to be considered in their implementation. Some disadvantages of AC microgrids include loss of power in voltage conversion, limited use of renewable resources, lower efficiency over long distances, difficulty coping with demand peaks, and limited voltage flexibility [52]–[54].

DC microgrids are a type of decentralized energy system that uses direct voltage and current in energy distribution and storage. DC microgrids have several advantages that make them an attractive option in some contexts. Following are some of the advantages of DC microgrids. High energy efficiency, Easy integration with renewable resources, maintenance of DC equipment, efficient energy storage, flexibility in design and implementation, ease of management and control, safety at consumer level, and suitable for Special applications such as data centers, street lighting systems, and electric vehicles. These advantages make DC microgrids an attractive option especially in scenarios involving renewable resources, energy storage, and the use of equipment that generally operates on DC voltage and current [55]–[57].

Droop control is a control method used in electric power systems, especially in microgrid systems or decentralized distribution systems [58], [59]. The aim of droop control is to maintain voltage and frequency stability in the electrical system when load fluctuations occur. This is important because large fluctuations in frequency or voltage can disrupt the operation of electrical equipment and cause damage to the system. This method can be applied to electrical generators and power converters in microgrids or distribution systems that operate independently. Specifically, droop control adjusts the device output in a manner that is proportional to the deviation of the voltage or frequency from a reference value. Droop control on converters is used to maintain voltage and frequency stability in decentralized power systems, such as microgrids. Power converters, especially those used on renewable resources such as solar panels or wind turbines, play an important role in integrating these resources into the electrical grid. Droop control in the converter helps maintain power balance in the system in a manner that is proportional to the voltage or frequency deviation [60]–[62].

Droop control in DC microgrids is a control method used to maintain voltage and frequency stability in microgrids that operate with direct voltage and current (DC). DC microgrid systems often consist of multiple renewable resources, energy storage, and loads connected in a decentralized network [62]–[64]. Conventional droop control devices are employed in a DC Microgrid to introduce virtual resistances, which serve to distribute currents. Fluctuations in the bus voltage can give rise to the problem [65]–[67]. Regulating voltage and current distribution poses a challenge in this scenario. In the context of voltage control, a low virtual resistance results in an evenly distributed current but inadequate voltage regulation. Conversely, a high virtual resistance leads to an evenly distributed current but robust voltage regulation. Moreover, the irregular line resistance impacts the distribution of voltage and current [68]–[70].

Conventional droop control systems have proven to be a convenient method in DC microgrids due to their lack of reliance on communication links. The cost-effectiveness and user-friendliness of this technology contribute to its widespread adoption in DC microgrids. The lack of accuracy in power distribution and inadequate voltage control of this approach, despite their seemingly conflicting objectives, impede its broad implementation [71], [72]. Traditional techniques yield inadequate regulation of the electrical current sent between converters, incorrect allocation of current, and excessive variations in voltage [73], [74]. The droop coefficient is the factor that determines the precision of voltage stability and power distribution [75], [76]. More precisely, the accuracy of the current division increases as the voltage fluctuation increases, and conversely, when the droop coefficient increases. Extensive study has been conducted to address the shortcomings of this control system [77]–[79]. Conventional droop control, although becoming standard in some applications, has several disadvantages that need to be considered: unresponsive to load changes, lack of precision in regulating voltage, load imbalance, limitations in handling disturbances, dependence on network configuration, susceptible to incorrect settings and lack of ability to cope with maximum load variations. With advances in technology and the need for more adaptive and responsive control in modern power systems, computational droop control is increasingly becoming an attractive option and can provide significant benefits.

Innovations in droop control for DC microgrids continue to develop as the complexity and needs of decentralized electricity distribution systems increase. Several technological innovations that occur in DC microgrid droop control: adaptive algorithms, integration of renewable energy sources, use of communication technology, energy storage integration, hierarchical control, use of artificial intelligence technology, development of dynamic models. These innovations contribute to the development of more efficient, reliable and adaptive droop control for dc microgrids, enabling better integration of renewable energy sources, increased reliability and higher operational efficiency in electricity distribution systems [80], [81].

Metaheuristic optimization methods are approaches used to find optimal solutions or close to optimal solutions in large and complex search spaces. Metaheuristics are search techniques that are independent of the specific problem and tend to be effective for global optimization problems. Several new metaheuristic methods have been presented that are similar in application function as optimization techniques. One-to-One Based Optimizer (OOBO) is a new optimization technique for solving optimization problems in various scientific fields. The key idea in designing the suggested OOBO is to effectively use the knowledge of all members in the process of updating the algorithm population while avoiding the algorithm depending on certain population members. one-on-one correspondence between two groups of population members and selected members as a guide to increasing the involvement of all population members in the updating process. The CEC 2017 test suite which include fixed-dimensional, high-dimensional, and unimodal multimodal types are used to assess the optimization performance of the OOBO. The optimization findings demonstrate OOBO's amazing ability to balance exploration and exploitation in the problem-solving space while conducting a search [82].

The Preschool Educational Optimization Algorithm (PEOA), a novel human-based metaheuristic algorithm, is proposed to solve optimization problems. The involvement of humans in the preschool education process serves as a major source of inspiration for the design of PEOA. PEOA is mathematically modeled in three phases: (i) the steady increase of preschool teacher educational influence, (ii) the teacher-guided development of individual knowledge, and (iii) the increase in individual knowledge and self-awareness. The CEC 2017 test suite was used to evaluate PEOA's optimization potential. The optimization results that were obtained demonstrated how well PEOA balanced local exploitation and global exploration during the search. The PEOA technique for global optimization issues offers a number of benefits. In contrast to these benefits, PEOA has a number of drawbacks. The primary benefit of PEOA lies in its mathematical model's absence of control parameters that require human adjustment. Like all stochastic based optimizers, PEOA's primary drawback is that it cannot be guaranteed to find the global optimal solution [83].

The Red-Tailed Hawk Algorithm (RTH) is a novel metaheuristic optimization technique inspired by nature. The red-tailed hawk, being a predator, employs a hunting technique that encompasses the detection of prey to the swooping stage. The hunting procedure consists of three distinct stages. During the elevated flight phase, the red-tailed hawk actively investigates the search area and identifies the specific location of its prey. During the low soaring stage, the red-tailed hawk maneuvers within the designated area surrounding its prey to strategically select the optimal position for hunting. Subsequently, the red-tailed bird swiftly swings and successfully strikes its intended objective throughout the descending and gliding phases. The suggested approach emulates the hunting strategy of the red-tailed hawk to solve practical optimization challenges. Twenty-three common benchmark test functions are used to evaluate RTH performance. These three types of mathematical functions help identify the nature of various optimization issues. The findings demonstrate that the suggested algorithm can quickly and robustly find the best solution for the majority of the functions under consideration [84].

Several metaheuristic applications in droop control have been presented by several researchers. A novel droop control technique is given, which enhances the optimization of particle swarms in island microgrids with many distributed generations operating in parallel. The incorporation of a fuzzy inference system enhances the original particle swarm optimization technique by dynamically adapting its parameters, resulting in enhanced convergence speed and optimization precision [85]. A new droop control approach is implemented by utilizing a proportional resonant (PR) controller, with its proportional gain optimized through the Ant Lion Optimization algorithm (ALO). The ALO optimized PR controller outperforms the typical PI controller in terms of error indices, voltage regulation, speed of response, and T.H.D levels [86]. The most suitable pairing of DC side capacitance (C) and PI gain is determined by employing the computational power of the swarm salp optimization algorithm (SSA), which is one of the most sophisticated soft computing optimization techniques available. This ideal combination ensures a suitable transient response when there are changes in load circumstances and when a distributed generator (DG) is added. The efficacy of the recommended control strategy is evaluated by comparing the results with previous methods that rely on transient response measurements, solution quality, and power quality, which have been used in recent research [87].

Although many metaheuristic algorithms have been proposed to optimize droop control, further research is needed to achieve optimal droop control performance for various types of problems. Therefore, this work offers an improved and modified droop control that uses the Lévy flight and the Osprey optimization algorithm (OOA) method. This article makes the following contributions:

1. Modification of the Osprey optimization algorithm (OOA) by adding the Lévy flight algorithm known as MOOA. The Lévy Flight algorithm has several advantages including search efficiency, ability to find the global optimum and adaptability to the environment.
2. Modify droop control by applying PID to secondary control. PID (Proportional-Integral-Derivative) is an extension of the simpler PI (Proportional-Integral) control. Some of the advantages of PID compared to PI

control are faster response, reduced overshoot, ability to handle non-linear systems and better stability

3. Using the 23 CEC2017 Benchmark function, the performance of MOOA in solving optimization problems is assessed and compared with One-to-One Based Optimizer (OOBO), Preschool Educational Optimization Algorithm (PEOA) and Red-Tailed Hawk Algorithm (RTH). The benchmark function is designed to provide an objective evaluation standard for optimization algorithms, such as genetic algorithms, swarm algorithms, and other evolutionary algorithms.
4. To determine the performance of implementing PID optimized with MOOA in a DC microgrid system compared with PI.

The structure of this article is as follows: the Osprey optimization algorithm, Lévy Flight, Droop Control, and Proportional Integral Derivative (PID) are described in Section 2. Section 3 is the recommended control scheme. In Section 4 there are discussions and simulations. The conclusion is presented in the last section.

II. METHODS

A. Droop Control

The main function of droop control in DC microgrids is to ensure balanced power distribution between power sources and loads in the microgrid when load changes occur. This helps maintain voltage stability. When load changes occur in a DC microgrid, droop control ensures that available resources contribute proportionally to those changes [88], [89]. This helps prevent power imbalances between resources and ensures that each resource makes an appropriate contribution to load requirements. Droop control helps maintain voltage within the desired range when load changes occur. This can avoid significant voltage fluctuations and maintain the operational stability of the microgrid [90], [91].

DC microgrids often include renewable resources such as solar panels and wind turbines. Droop control helps integrate the variable output of these renewable resources in a stable and distributed manner [92]. Applying droop control to DC microgrids can help create adaptive and efficient systems, especially in the context of small distributed power grids. By maintaining balanced power distribution, droop control supports the stable and reliable performance of DC microgrids [93].

The analogous circuit for two dc power supply is depicted in Fig. 1. linked in parallel and using resistive output impedances to share a shared load. A current will flow between the two dc sources if there is a voltage difference. Using a primary control, we can program virtual output impedances to lower the circulating current. The inner current and voltage control loops' voltage reference is modified by this control level (level 0). It has the output voltage stated as follows in the virtual output impedance loop:

$$V^*_o = \mathrm{V}_{ref} - \left(\mathrm{R}_{dj} \cdot i_j\right); j = 1,2 \quad (1)$$

$$\mathrm{V}_{ref} = \mathrm{v}_{DCn} - \varepsilon_v/2 \quad (2)$$

With the assumption that the maximum allowable voltage deviation is ε_v, the following design guidelines for R_{dj} and V_{ref} ought to be applied.

$$\mathrm{R}_{dj} = \varepsilon_v/\mathrm{I}_{max} \quad (3)$$

V_{ref} is the DC bus voltage reference set point in this case. Droop coefficient, or virtual resistance, is $\mathrm{R}_{d,j}$. Whereas v_n is the nominal output voltage, I_{max} is the maximum output current.

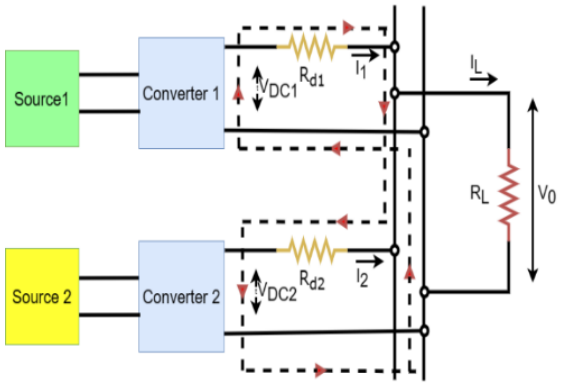

Fig. 1. DC Bus-connected parallel dc-dc converter

This control loop provides the power converter with a resistive output impedance to compensate for the variation between the reference voltages, $\Delta\mathrm{V}_o = \mathrm{V}_{o1} - \mathrm{V}_{o2}$. As a result, the formula for the two converters' respective current distribution is as follows:

$$\Delta\mathrm{I}_o = \mathrm{I}_{o1} - \mathrm{I}_{o2} \quad (4)$$

$$\Delta\mathrm{I}_o = \Delta\mathrm{V}_o/\mathrm{R}_{dj} \quad (5)$$

This control not only allows the converters to run in parallel but also improves the dynamic performance of the output voltage. However, the voltage difference varies with load. Voltage regulation and power sharing precision are subject to performance trade-offs implemented by the droop controller at the primary control layer. A variety of distributed, decentralized, and centralized methods have been developed in recent years within the hierarchical control framework to improve power sharing accuracy, compensate for voltage deviations, and improve the reliability of DC microgrids. The main disadvantage of using the droop control method is the appearance of voltage deviations in the DC bus voltage when the power generated, and power consumed have an inequality.

To minimize voltage deviations in the DC bus voltage, a level control secondary based on a PI (proportional-integral) controller is used to apply appropriate voltage deviation compensation δv. Secondary control is used to reduce voltage deviations. All dv_0 units get the error processed by the compensator to be able to compute the output voltage, which is established by monitoring the microgrid's voltage level and contrasting it with the reference voltage V^*_{MG} (see Fig. 2). The controller has made the following statement:

$$\mathrm{dv}_o = \mathrm{k}_p(V^*_{MG} - \mathrm{V}_{MG}) + \mathrm{k}_i \int (V^*_{MG} - \mathrm{V}_{MG})dt \quad (6)$$

Where k_p and k_i are the control settings of the compensator secondary control. Keep in mind that dv_o must be restrained to remain under the highest voltage deviation. Eq. (1) becomes at last.

$$V^*_o = \left(V^*_{ref} + \mathrm{dv}_o\right) - \mathrm{R}_d \cdot \mathrm{I}_o \quad (7)$$

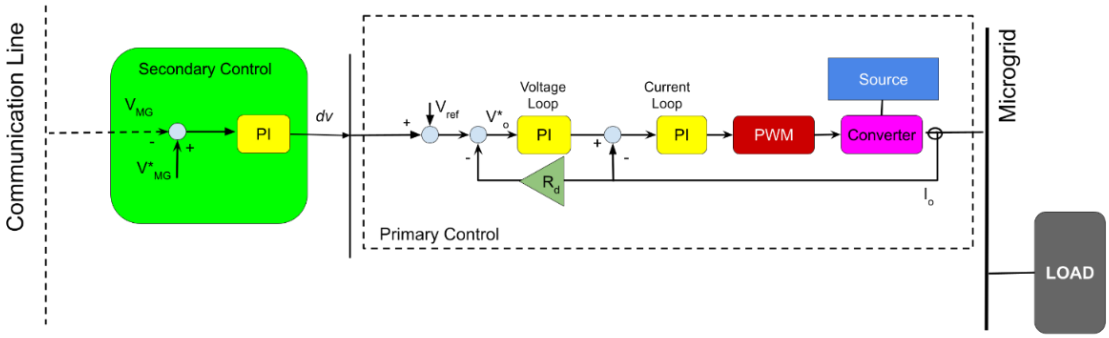

Fig. 2. Secondary and primary controls for DC microgrids

B. *Proportional Integral Derivative (PID)*

PID (Proportional, Integral, Derivative) control is one of the control methods used in automatic control systems[94]. The use of PID control in droop control provides significant effectiveness in regulating frequency and voltage in microgrid systems. Several practical examples of the effectiveness of PID in droop control have been presented. In DC microgrids that use renewable energy sources such as solar panels or wind turbines, PID control in droop control is used to regulate the power contribution from renewable energy sources into the system [95], [96]. In DC microgrids that use multiple inverters to generate power from renewable energy sources or energy storage, PID control in droop control can be used to efficiently coordinate inverter operation [97], [98].

The main function of PID control is to ensure that a system can reach and maintain its setpoint (desired value) as efficiently as possible [99]. Every each PID component serves a distinct purpose. The Proportional (k_p) control algorithm generates an output signal that is directly proportional to the deviation between the desired setpoint value and the current value of the system. In this scenario, the magnitude of the output signal increases in direct proportion to the magnitude of the difference. This component enhances the system's responsiveness to changes and brings it closer to the desired setpoint value.

The integral (k_i) is a measure of the cumulative difference between the setpoint value and the actual value of the system over a period. Integrals are useful for mitigating persistent defects in a system, even when the proportional components have already provided a response. This facilitates the system in achieving the designated setpoint value with accuracy and punctuality.

The derivative (k_d) measures the pace at which the difference between the setpoint value and the actual value of the system changes. The inclusion of derivative components in the system aids in achieving a seamless response to sudden alterations, hence avoiding the occurrence of overshooting (i.e., surpassing the desired value) or excessive oscillations.

In essence, PID operates by integrating these three elements to generate an ideal output signal for system control. The PID parameters (k_p, k_i, and k_d) can be fine-tuned based on the unique attributes and requirements of the controlled system. An optimally calibrated system utilising PID control can attain stability, accuracy, and excellent responsiveness to dynamic situations or desired values. An illustration of the Proportional Integral Derivative can be seen in Fig. 3. The PID equation is shown in Eq. 8.

$$\mathrm{G}_{pid}(s) = \mathrm{u(t)} = \mathrm{k}_p e(t) + \mathrm{k}_i \int e(t)dt + \mathrm{k}_d \frac{de(t)}{dt} \quad (8)$$

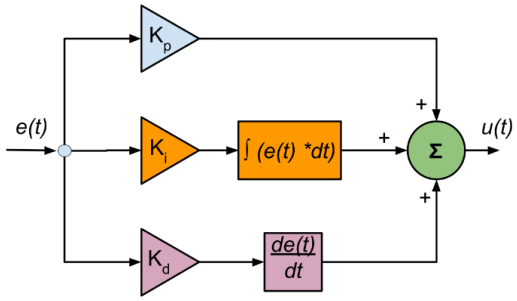

Fig. 3. PID Controller

C. *Osprey Optimization Algorithm*

Osprey Optimization Algorithm (OOA) is an algorithm that imitates the natural behavior of ospreys [100]. random starting position in the search space at the start of the OOA implementation using Eq. (9).

$$X = \begin{bmatrix} X_1 \\ \vdots \\ X_i \\ \vdots \\ X_N \end{bmatrix}_{Nxm} = \begin{bmatrix} X_{1,1} & \cdots & X_{1,2} & \cdots X_{1,m} \\ \vdots & \ddots & \vdots & \vdots \\ X_{i,1} & \cdots & X_{i,j} & \cdots X_{i,m} \\ \vdots & \vdots & \vdots & \ddots \\ X_{N,1} & \cdots & X_{N,j} & \cdots & X_{N,m} \end{bmatrix}_{Nxm} \quad (9)$$

$$X_{i,j} = lb_j + r_{i,j} \cdot \left(ub_j - lb_j\right) \quad (10)$$

Where X is the osprey population matrix, X_i is the i^{th} osprey (possible resolution). $X_{i,j}$ is the j^{th} size (variables pertaining to the problem), N is the quantity of ospreys, m is the number of variable problems. $r_{i,j}$ is a random number in the interval [0, 1], lb_j is the lower bound and ub_j is the upper bound. Eq.

(3) states that the evaluated values for the problem's objective function can be represented by a vector.

$$F = \begin{bmatrix} F_1 \\ \vdots \\ F_i \\ \vdots \\ F_N \end{bmatrix}_{Nxm} = \begin{bmatrix} F(X_1) \\ \vdots \\ F(X_i) \\ \vdots \\ F(X_N) \end{bmatrix}_{Nxl} \quad (11)$$

Where F is an objective function values vector and F_i is the value of the objective function found for the i^{th} osprey.

1) Phase 1: Fish hunting (exploration) and position identification.

An underwater fish is defined in the OOA design as the position of another osprey in the search space with a higher objective function value for each osprey. Using the Eq. (12), the fish assemblage for each osprey was found.

$$FP_i = \{X_i | k \in \{1,2,\dots,N\} \wedge F_k < F_i\} \cup \{X_{best}\} \quad (12)$$

$$X_{i,j}^{PI} = x_{i,j} + r_{i,j} \cdot \left(SF_{i,j} - I_{i,j} \cdot x_{i,j}\right) \quad (13)$$

$$X_{i,j}^{PI} = \begin{cases} X_{i,j}^{PI}, & lb_j \le X_{i,j}^{PI} \le ub_j; \\ lb_j, & X_{i,j}^{PI} < lb_j; \\ lb_j, & X_{i,j}^{PI} > lb_j; \end{cases} \quad (14)$$

$$X_i = \begin{cases} X_i^{PI}, & F_i^{PI} < F_i \\ X_i, & else \end{cases} \quad (15)$$

Where FP_i is the set of fish positions for i^{th} osprey and X_{best} is the greatest osprey (or contender) solution. One of these fish is randomly located by the osprey, which then strikes it. Eq. (13) is used to determine the updated location of the relevant osprey based on the osprey's simulated movement towards the fish. According to the Eq. (15), the osprey's original position is replaced by this new one if it raises the value of the objective function. X_i^{PI} is the prey's new location depending on the initial OOA phase. $X_{i,j}^{PI}$ is its j dimension, $r_{i,j}$ is a random number in the interval [0, 1], and $I_{i,j}$ is a random number from the set {1, 2}., F_i^{PI} is the objective function value, SF_i is the fish selected for the i^{th} prey, $SF_{i,j}$ is the j dimension

2) Phase 2: Fishing them into the right spot (exploitation).

In Phase 2, a new random position is calculated as a position suitable for fish feeding using Eq. (16). If the value of the goal function remains constant at this new position, it will replace the old position of the associated osprey according to Eq. (17).

$$X_{i,j}^{P2} = x_{i,j} + \frac{lb_j + r \cdot \left(ub_j - lb_j\right)}{t}; \; i = 1,2,\dots,N; j = 1,2,\dots,m; \; t = 1,2,..T \quad (16)$$

$$X_{i,j}^{P2} = \begin{cases} X_{i,j}^{P2}, & lb_j \le X_{i,j}^{P2} \le ub_j; \\ lb_j, & X_{i,j}^{P2} < lb_j; \\ lb_j, & X_{i,j}^{P2} > lb_j; \end{cases} \quad (17)$$

$$X_i = \begin{cases} X_i^{P2}, & F_i^{P2} < F_i \\ X_i, & else \end{cases} \quad (18)$$

Where X_i^{P2} is the new position of the prey based on the second phase of OOA. $X_{i,j}^{P2}$ is the j^{th} dimension. F_i^{P2} is the value of the objective function. $SF_{i,j}$ is the fish selected for the i^{th} prey. $SF_{i,j}$ is the j dimension. $r_{i,j}$ is a random number in the interval [0, 1]. t is the iteration counter of the algorithm, and T is the total number of iterations.

All the osprey positions were updated in accordance with the first and second stages of the intended OOA, completing the first iteration. Next, a comparison of the objective function values led to modifications to the best candidate solution. After that, the algorithm went on to the iteration that used the updated osprey placements, and so on, ending with the final iteration that used Equation (12) to (18). After the method has been fully implemented, the best candidate solution that was stored during the iterations is eventually given as a solution to the problem.

A. Lévy Flight Optimization

Lévy flight is a particular class of general random walks in which the stride length during the walk is described by a heavy-tailed probability distribution [101]. They can describe all stochastic processes that are scale-invariant.

$$L(X_j) \approx \left|X_j\right|^{1-\alpha} \quad (19)$$

Where X_j is the flight length, and $1 < \alpha \le 2$ is the exponential power. The probability density of the Lévy stable process in integral form is defined as Eq. (12).

$$f_L(x;\alpha,\gamma) = \frac{1}{\pi}\int_0^\infty exp(-\gamma q^\alpha)\cos\,(qx)\;dq \quad (20)$$

Where α is the distribution index and controls the scale properties of the process while γ selects the scale units. Integrals in Eq. (11) have an analytical solution only in some cases. When α equals 2, it represents a Gaussian distribution and when α equals 1, it represents a Cauchy distribution. The solution to the integral in Eq. (11) generally requires the use of the series expansion method only when x has very large values as Eq. (13):

$$f_L(x;\alpha,\gamma) = \frac{\gamma\Gamma(1+\alpha)\sin(\frac{\alpha\pi}{2})}{\pi X^{(1+\alpha)}}, x \to \infty \quad (21)$$

Where Γ is Gamma function. Mantegna[102]proposed an accurate and fast algorithm to generate stable Lévy processes for absolute values of the index distribution (α) ranging between 0.3 and 1.99. Mantegna's method for random number generation is based on the Lévy distribution in Eq.14

$$Levy(\alpha) = 0.05 \times \frac{x}{|y|^{1/\alpha}} \quad (22)$$

$$x = Normal\,(0,\sigma_x^2) \quad (23)$$

$$y = Normal\,(0,\sigma_x^2) \quad (24)$$

$$\sigma_x = \left[\frac{\Gamma(1+\alpha)\sin(\frac{\alpha\pi}{2})}{\Gamma\left(\frac{(1+\alpha)}{2}\right)\alpha\, 2^{\frac{(\alpha-1)}{2}}}\right]^{1/\alpha} and\ \sigma_x = 1 \text{ dan } \alpha = 1.5 \quad (25)$$

Where x and y are two normally distributed variables with standard deviations σ_x and σ_y. The application of the Lévy flight algorithm is used as a search tool to optimize

parameters in droop control. This includes adjustment of droop constants, and coordination between control components to achieve optimal performance in terms of system stability, efficiency, and response. in addition, the Lévy flight algorithm could make dynamic adjustments to environmental conditions and operational needs of the microgrid. This allows droop control to be more adaptive to load changes, resource fluctuations, or network disruptions, thereby improving overall system reliability and performance. With the right approach, this algorithm can help overcome control challenges in microgrids.

III. PROPOSED METHODS

A. Modified Osprey Optimization Algorithm (MOOA)

Osprey optimization algorithm (OOA) can solve low-dimensional an unimodal optimization problems easily. However, when dealing with high-dimensional and multimodal optimization problems, the solutions obtained by OOA are not so good. To improve exploration, local optimal avoidance, exploitation, and OOA convergence, the Modified Osprey optimization algorithm (MOOA) algorithm is proposed. The proposed method combines the Osprey optimization algorithm (OOA) and Lévy flight optimization. Lévy flight optimization can maximize search agent diversification, which ensures that the algorithm can explore the search field efficiently and achieve minimum local avoidance. Lévy flight trajectories are helpful in getting a better move from exploration to exploitation in OOA.

Therefore, the Lévy flight trajectory is used to update the Osprey's position after the position update. Fig. 4 is an MOOA flow diagram. The proposed MOOA method is a modification of the OOA method by changing Eq. (8) and adding Eq. (14) to Eq. (8). So, it becomes the following:

$$X_{i,j}^{P2} = x_{i,j} \frac{Levy(\alpha)}{t}\ ;\ i = 1,2,\dots,N; j = 1,2,\dots,m;\ t = 1,2,..T \quad (26)$$

Ospreys carry the fish they catch to good locations to eat them. Based on this simulation of real behavior, the second phase of population updating in standard OOA is modeled. The position of the osprey in the search space is created by small changes caused by modeling the transport of the fish to the right position, which increases the power of OOA exploitation in local search and causes convergence towards a better limited solution. Modifying OOA by adding the levy algorithm in the exploitation phase produces small and sometimes large steps or long-distance jumps to expand the search space and improve global search capabilities, even to speed up the convergence speed. Lévy flight steps are used to update the position.

B. Modified Secondary Control

In a microgrid system, secondary control in droop control is used to improve overall system performance by paying attention to interactions between connected units. Several important aspects of secondary control in modified droop control are that it allows better coordination between units in the microgrid, can improve voltage and frequency effectively in the microgrid by suppressing overshoot and speeding up recovery of transient conditions, and allows the system to respond quickly to disruptions and unexpected changes in conditions. This research presents the latest approach to secondary control using PID. PI control systems tend to have overshoot (more than the setpoint value) and oscillation, especially if the integral gain (Ki) value is too large. This can cause the system to overshoot the target before finally settling around the setpoint value. Selection and adjustment of control parameters, as well as the introduction of additional control elements such as Derivative (D) in PID (Proportional-Integral-Derivative) control, can help overcome some of these disadvantages. So Eq. (6) becomes Eq. (27).

$$dv_o = k_p(V^*_{MG} - V_{MG}) + k_i \int (V^*_{MG} - V_{MG})dt + k_d \frac{d(V^*_{MG} - V_{MG})}{dt} \quad (27)$$

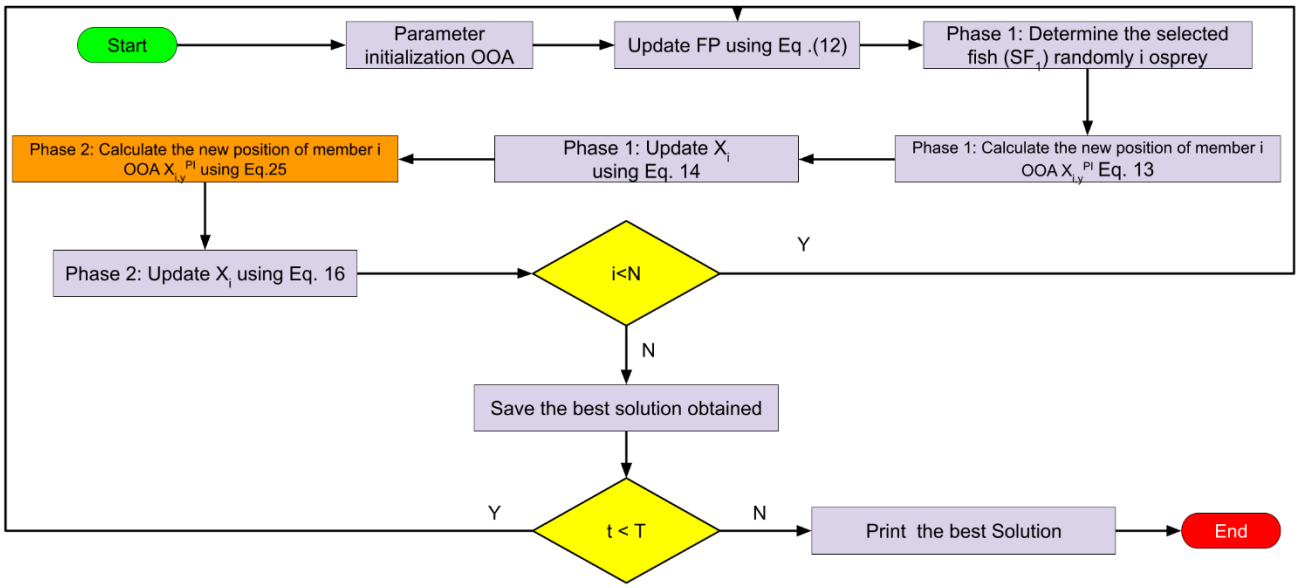

Fig. 4. The flow diagram of MOOA

IV. RESULTS AND DISCUSSION

A. Convergence Curve Profile

The results of the proposed MOOA approach are compared to those of existing advanced techniques, including the Preschool Education Optimization Algorithm (PEOA), Red-Tailed Hawk Algorithm (RTH), One-to-One Based Optimizer (OOBO), and OOA. This article assesses the performance of MOOA by use the benchmark function. Initially, it is necessary to consider the 23 CEC2017 benchmark functions. The function F1–F7 is characterized as unimodal. The function F8–F13 is multimodal. F14-F23 refers to fixed-dimensional multimodal functions that are represented by mathematical equations. The simulation is executed via the MATLAB/Simulink program. Fig. 5 presents a comparison of the outcomes of benchmark functions using the algorithms PEOA, RTH, OOBO, OOA, and MOOA.

Statistical analysis is presented on the performance of MOOA and competitor algorithms to determine whether MOOA has a significant statistical advantage or not. By knowing the rank of each function, the mean rank value for each algorithm is obtained. Table I shows the statistical analysis of each function. The rank is a number indicating the best of mean value. The total rank value of each algorithm shows that MOOA has a value of 1. The average rank value is 1.739130435. Meanwhile, the difference in the Mean rank value between ranks 2, 3, and 4 is very slight. Table II is a comparison of the ranks of the unimodal functions of the algorithm. MOOA in multimodal has a rank of 1. A comparison of the multimodal function ranks of all the algorithms used can be seen in Table III. The MOOA and OOA rank values are the same, namely 1. In Table IV, the fixed-multimodal rank comparison of MOOA is 1. Comparison and characteristics of the solution distribution of each algorithm when solving 23 CEC2017 benchmark functions are shown in Fig. 5. The MOOA presented in this study outperforms its competitors in F1, F2, F3, F4, F6, F9, F10, F11, F12, F14, F15, F17, F18, F19, and F23. On F5, OOA has the best performance. PEOA has the lowest curve at F7.

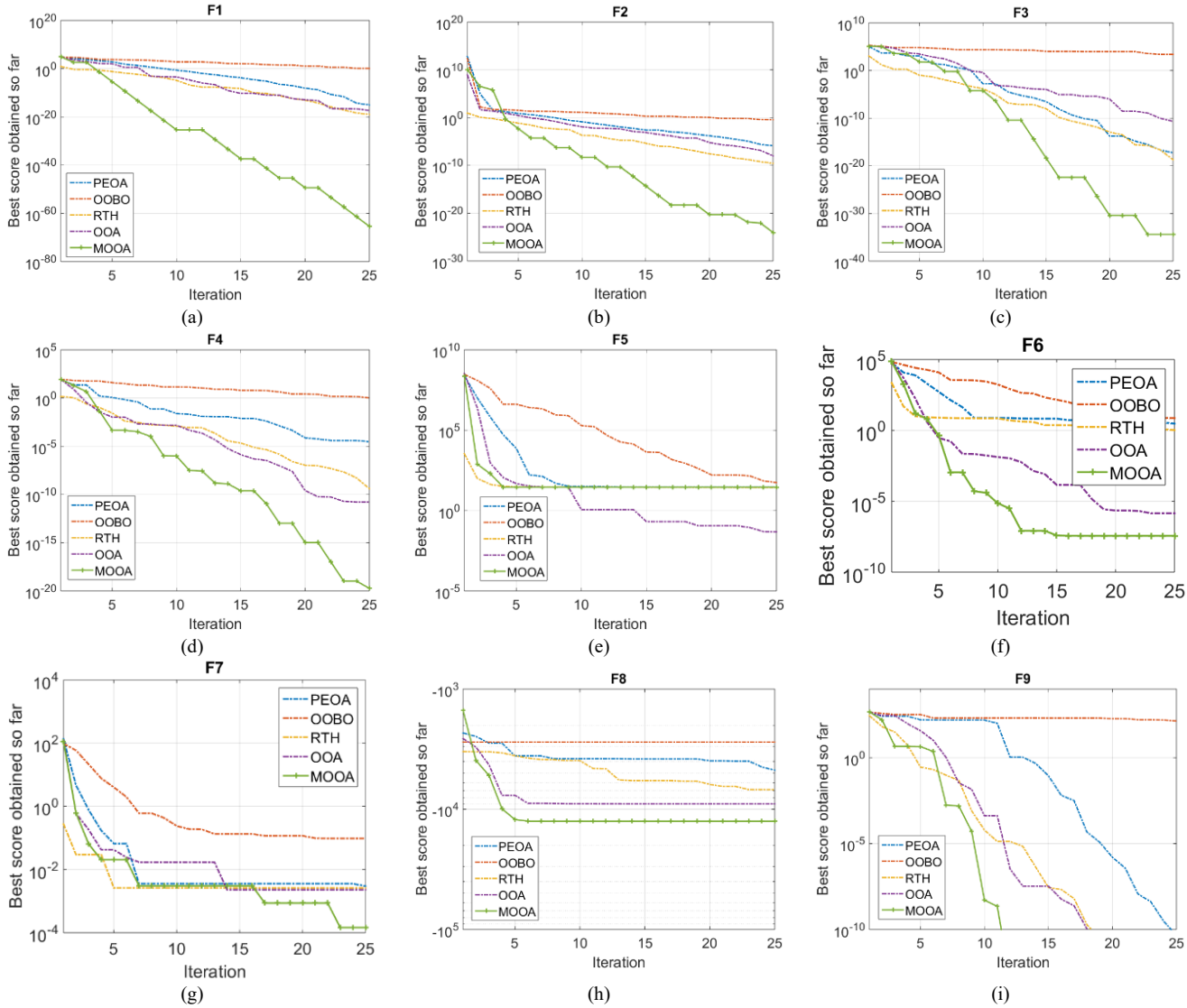

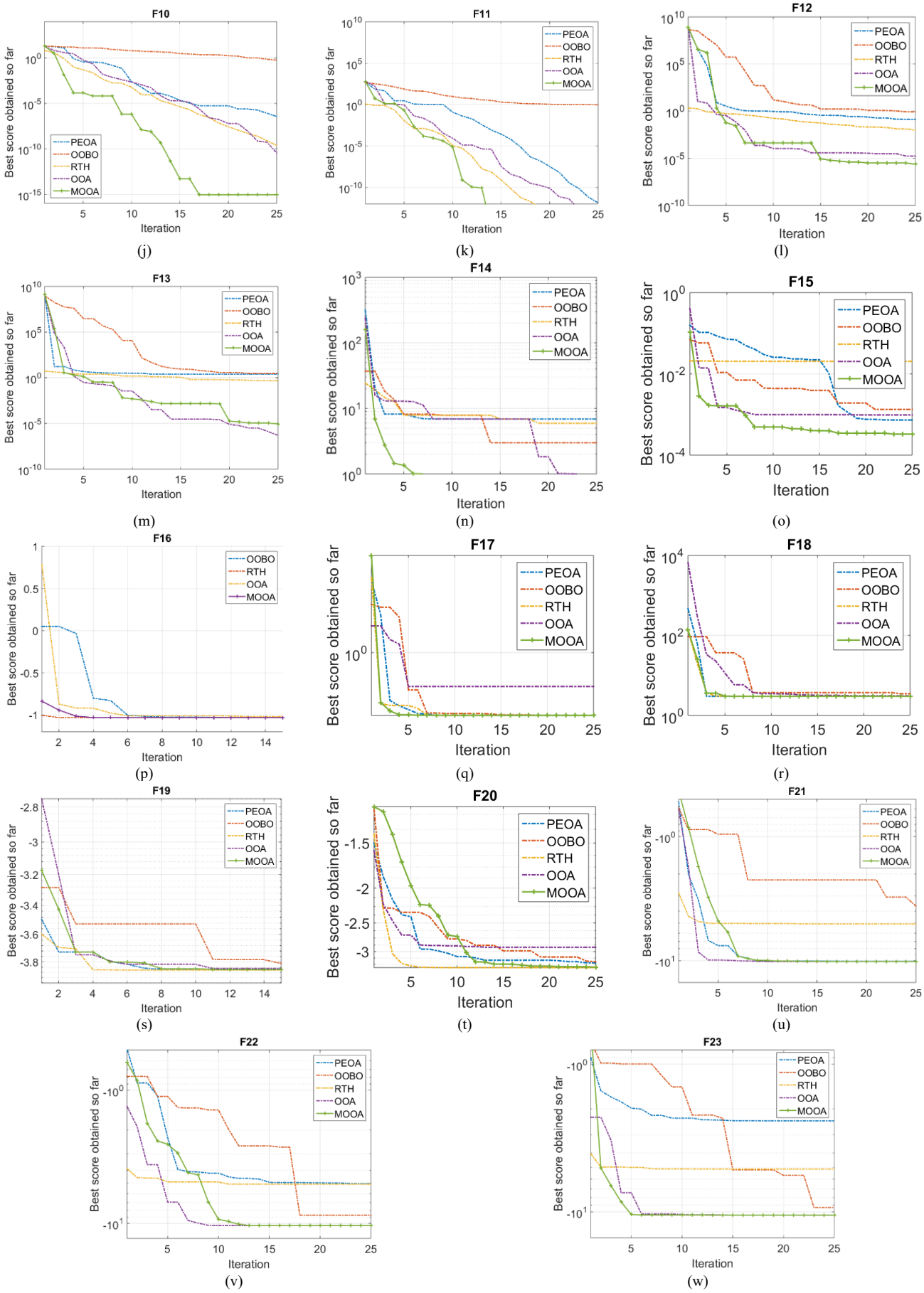

Fig. 5. Algorithm convergence curves on corresponding benchmark tests

TABLE I. COMPARISON OF MOOA AND OTHER ALGORITHMS

Function		OOBO	RTH	MOOA	OOA	PEOA
F1	Best	0.030547	2.60E-28	1.59E-77	2.77E-24	1.11E-26
	Mean	0.146	1.14E-20	1.65E-48	2.26E-18	1.11E-26
	Worst	0.44121	2.77E-19	4.07E-47	4.58E-17	1.11E-26
	Std	0.10134	5.54E-20	8.14E-48	9.11E-18	0
	Rank	5	4	1	3	2
F2	Best	0.088744	1.01E-13	4.46E-33	6.93E-13	2.04E-10
	Mean	0.159	8.76E-12	4.06E-23	4.23E-10	2.04E-10
	Worst	0.23641	6.91E-11	7.47E-22	2.97E-09	2.04E-10
	Std	0.038734	1.87E-11	1.51E-22	7.13E-10	0
	Rank	5	3	1	2	4
F3	Best	139.8532	2.02E-27	7.77E-74	1.61E-21	3.41E-24
	Mean	778.552	2.82E-21	1.76E-35	5.99E-10	3.41E-24
	Worst	2230.216	3.51E-20	3.93E-34	1.01E-08	3.41E-24
	Std	476.9595	9.30E-21	7.87E-35	2.14E-09	0
	Rank	5	3	1	4	2
F4	Best	0.32297	5.79E-14	8.74E-43	1.04E-13	4.81E-11
	Mean	0.51902	2.43E-12	2.48E-25	6.34E-11	4.81E-11
	Worst	0.86767	2.44E-11	3.68E-24	4.58E-10	4.81E-11
	Std	0.1336	5.82E-12	8.02E-25	1.12E-10	0
	Rank	5	2	1	3	4
F5	Best	29.6128	26.1362	4.27E-05	9.23E-11	28.8952
	Mean	31.4232	27.6911	24.943	0.0085848	28.8952
	Worst	35.6354	28.7012	28.7746	0.15201	28.8952
	Std	1.6964	0.57252	9.2894	0.032311	0
	Rank	5	3	2	1	4
F6	Best	3.9134	0.15036	1.06E-08	1.91E-12	2.3445
	Mean	5.1959	0.47326	0.012117	8.22E-05	2.3445
	Worst	6.0357	0.97497	0.042418	0.0006521	2.3445
	Std	0.54007	0.24345	0.011621	0.000195	0
	Rank	5	3	2	1	4
F7	Best	0.0060617	0.0001208	4.81E-05	3.43E-05	0.0030057
	Mean	0.020848	0.0013852	0.0019676	0.0014177	0.0030057
	Worst	0.0718	0.0038596	0.0059192	0.0039102	0.0030057
	Std	0.013792	0.0009004	0.0016135	0.0011241	0
	Rank	5	2	3	1	4
F8	Best	-4237.0406	-8728.8512	-12569.487	-12569.487	-5621.781
	Mean	-3252.0579	-7285.6639	-9603.9426	-10436.006	-5621.781
	Worst	-2588.8041	-6351.0867	-3533.8006	-9016.0058	-5621.781
	Std	408.4557	594.5367	2962.6224	1774.6349	0
	Rank	5	3	2	1	4
F9	Best	2.8225	0	0	0	186.6653
	Mean	20.0082	0	0	0	186.6653
	Worst	53.3647	0	0	0	186.6653
	Std	16.065	0	0	0	0
	Rank	2	1	1	1	3
F10	Best	0.079224	7.99E-15	8.88E-16	9.68E-14	2.69E-11
	Mean	0.12849	8.83E-13	8.88E-16	5.21E-11	2.69E-11
	Worst	0.18116	6.79E-12	8.88E-16	4.79E-10	2.69E-11
	Std	0.032135	1.64E-12	0	9.77E-11	0
	Rank	5	3	1	2	4
F11	Best	0.10736	0	0	0	0
	Mean	0.32278	0	0	0	0
	Worst	0.66857	0	0	0	0
	Std	0.12994	0	0	0	0
	Rank	2	1	1	1	1
F12	Best	0.35508	0.0055156	9.93E-19	2.66E-13	0.11754
	Mean	0.61088	0.020033	6.97E-06	1.75E-06	0.11754
	Worst	0.84813	0.041693	4.51E-05	1.70E-05	0.11754
	Std	0.11753	0.010779	1.25E-05	4.82E-06	0
	Rank	5	3	1	2	4
F13	Best	2.3374	0.44964	1.29E-09	1.78E-12	2.9842
	Mean	2.9314	1.9696	0.13941	5.80E-06	2.9842
	Worst	3.3235	2.9693	1.3318	4.81E-05	2.9842
	Std	0.23085	0.93368	0.27585	1.28E-05	0
	Rank	5	3	2	1	4
F14	Best	1.0825	0.998	0.998	0.998	6.9033
	Mean	3.7183	4.098	3.0766	1.7642	6.9033
	Worst	9.6285	10.7632	12.6705	6.9033	6.9033
	Std	1.7705	3.7692	3.5096	1.4263	0
	Rank	3	4	2	1	5

Function		OOBO	RTH	MOOA	OOA	PEOA
F15	Best	0.0006802	0.0003075	0.0003079	0.0003196	0.0007287
	Mean	0.0018641	0.007723	0.0012145	0.0007695	0.0007287
	Worst	0.021132	0.020363	0.022267	0.0016383	0.0007287
	Std	0.0040299	0.009683	0.0043861	0.0004392	0
	Rank	4	5	3	2	1
F16	Best	-1.0316	-1.0316	-1.0316	-1.0316	-1.0316
	Mean	-1.03165	-1.03164	-1.03161	-1.0317	-1.03162
	Worst	-1.0313	-1.0316	-1.0316	-1.0282	-1.0316
	Std	0.0001012	4.53E-16	5.51E-06	0.001017	0
	Rank	4	3	1	5	2
F17	Best	0.3979	0.39789	0.39789	0.39789	0.39789
	Mean	0.39915	0.397891	0.39789	0.40271	0.39799
	Worst	0.40598	0.39795	0.3979	0.47168	0.39789
	Std	0.0019329	1.29E-05	2.56E-06	0.014991	0
	Rank	4	2	1	5	3
F18	Best	3	3	3	3	3
	Mean	3.0221	3	11.6406	4.1503	3
	Worst	3.4313	3	30.0017	30.004	3
	Std	0.085529	2.92E-14	12.8547	5.3884	0
	Rank	4	2	1	5	3
F19	Best	-3.8628	-3.8628	-3.8628	-3.8603	-3.8624
	Mean	-3.8613	-3.8319	-3.8624	-3.7647	-3.86241
	Worst	-3.8514	-3.0898	-3.8609	-3.2893	-3.8624
	Std	0.002915	0.1546	0.0003556	0.11177	0
	Rank	3	2	4	1	5
F20	Best	-3.3197	-3.322	-3.3195	-3.2932	-3.3199
	Mean	-3.2437	-3.2602	-3.2753	-2.4182	-3.3199
	Worst	-2.9996	-3.2031	-3.162	-1.59	-3.3199
	Std	0.069747	0.060624	0.059926	0.44798	0
	Rank	4	2	3	5	1
F21	Best	-9.1563	-10.1532	-10.1532	-10.1532	-10.1486
	Mean	-5.3591	-5.473	-7.1289	-10.1528	-10.1486
	Worst	-3.4018	-2.6305	-2.6827	-10.1451	-10.1486
	Std	1.4626	2.5498	3.073	0.0016129	0
	Rank	5	4	3	1	2
F22	Best	-10.2226	-10.4029	-10.4029	-10.4029	-5.0843
	Mean	-6.2031	-6.1776	-7.4178	-10.3994	-5.0843
	Worst	-3.1203	-2.7659	-1.8375	-10.3721	-5.0843
	Std	2.4428	2.505	3.0216	0.0087709	0
	Rank	3	4	2	1	5
F23	Best	-10.2725	-10.5364	-10.5364	-10.5364	-3.8346
	Mean	-7.5192	-5.9055	-17.2815	-10.5361	-3.8346
	Worst	-2.4036	-2.4217	-2.8707	-10.5322	-3.8346
	Std	2.5849	2.4765	3.2939	0.0008277	0
	Rank	3	4	1	2	5
F16	Best	-1.0316	-1.0316	-1.0316	-1.0316	-1.0316
	Mean	-1.03165	-1.03164	-1.03161	-1.0317	-1.03162
	Worst	-1.0313	-1.0316	-1.0316	-1.0282	-1.0316
	Std	0.0001012	4.53E-16	5.51E-06	0.001017	0
	Rank	4	3	1	5	2
Sum rank		96	66	40	51	76
Mean rank		4.173913043	2.869565217	1.739130435	2.217391304	3.304347826
Total rank		5	3	1	2	4

TABLE II. RANK COMPARISON OF UNIMODAL FUNCTIONS BETWEEN ALGORITHMS (F1-F7)

Function	OOBO	RTH	MOOA	OOA	PEOA
Sum rank	35	20	11	15	24
Mean rank	5	2.8571429	1.5714286	2.1428571	3.4285714
Total rank	5	3	1	2	4

TABLE III. RANK COMPARISON OF MULTIMODAL FUNCTIONS BETWEEN ALGORITHMS (F8-F13)

Function	OOBO	RTH	MOOA	OOA	PEOA
Sum rank	24	14	8	8	20
Mean rank	4	2.333	1.3333	1.3333	3.33
Total rank	4	2	1	1	3

TABLE IV. RANK COMPARISON OF FIXED-MULTIMODAL FUNCTIONS BETWEEN ALGORITHMS (F14-F23)

Function	OOBO	RTH	MOOA	OOA	PEOA
Sum rank	37	32	21	28	32
Mean rank	3.7	3.2	2.1	2.8	3.2
Total rank	4	3	1	2	3

B. Implementing MOOA for Droop Control

The DC microgrid depicted in Fig. 6 consists of two sources: a DC generator (DCG) and a photovoltaic (PV) system. A microgrid operates at a low voltage level, specifically with a bus voltage of 100V. Low voltage is commonly employed in residential installations to power DC loads. The specifics of the utilized system are displayed in Table I. An error arises from the differentiation between the bus voltage and the reference voltage, as depicted in Fig. 1. The absolute value is calculated, multiplied by the duration, and thereafter converted to ITAE. The MOOA iteration is iterated using the ITAE outcomes. The droop coefficient values for each converter and the PID parameters are included in the MOOA iteration results. Due to the temporal multiplication function of time multipliers, Integral of Time-weighted Absolute Error (ITAE) is useful for evaluating system performance in adapting to changes in setpoint or operational conditions. Therefore, ITAE is optimized in this study. The mathematical definition of ITAE is as follows:

$$ITAE = \int_0^\infty t.e(t).dt \quad (28)$$

Apart from that, to find out the reliability and stability of the system against control responses due to changes. This research uses ITSE (Integral of Time multiplied by Squared Error). The mathematical equation is as follows:

$$ITSE = \int_0^\infty t.e(t)^2.dt \quad (29)$$

In this session, the MOOA method combined with PID (MOOA-PID) for secondary control is presented. The performance of MOOA-PID is validated using the MOOA-PI method. The control parameters of the main control and secondary control are searched using the proposed method. The control parameters of the main control and secondary control are searched using the proposed method. The first comparison is a system without a second control and the second comparison is a system that has a second control. The parameters obtained from the MOOA approach are applied to the system. The parameters obtained can be seen in Table V and Table VI. Table V is the parameters in the first source and Table VI is the control parameters in the second source. Testing the application of the proposed method to droop control uses 3 case studies, namely:

1. The first case study is implementing the system with an initial load of 4000 W and in the 1st second the load drops by 500 W.
2. The second case study is a system with a load of 2500 W and the load increases by 800 W in the 1st second,
3. The third case study is a 3000W load system whose load conditions change. The load in the 1st minute increases by 1000W and decreases by 500W in the 2nd second.

In case study 1, the system has a load of 4000 W. In the 1st second, the system loses a load of 500 W. So, the system is loaded with a load of 3500 W. An illustration of the power, voltage and current of the system with the concept of case study 1 can be seen in Fig. 7. In the first case study, the average overshoot voltage of MOOA-PI and MOOA-PID is 118.15 and 106.9. The proposed method has an average overshoot voltage of 9.521%. Meanwhile, the proposed method can reduce the average undershoot voltage value by 3.35%. The performance in assessing the stability and precision of the control system measured using ITSE shows that the MOOA-PID method is 41.1738% better than the MOOA-PI method. Control response measurements to evaluate system performance in adapting to changes in setpoint or operational conditions using ITAE found that the MOOA-PI method had a better response of 7.11% compared to MOOA-PID. Detailed simulation results from case study 1 can be seen in Table VII.

In case study 2, the system load is 2500W which increases to 3300W in the 1st second. An illustration of the load changes in the system with case study 2 can be seen in Fig. 8. The average undershoot voltage value from the MOOA-PID method is 6.736% better than MOOA-PI. Meanwhile, the average value of Overshoot voltage for the MOOA-PID method is 8.522% better than MOOA-PI. The ITSE value of MOOA-PID is 17.742% better than MOOA-PI. Meanwhile, the ITAE value from MOOA-PI is 10.556% better than MOOA-PID. Details of the simulation with case study 2 conditions can be seen in Table VIII.

In the third case study, the system was conditioned by changing the load twice, namely by increasing the load by 1000W and decreasing the load by 500W. An illustration of the third case study can be seen in Fig. 9. From the simulation in the third case study, the ITSE value of MOOA-PID is 7.99% better than MOOA-PI. On the other hand, the ITAE value from MOOA-PI is 23.118% better than MOOA-PID. The average value of voltage overshoot from MOOA-PID has a better value of 11.707%. The average voltage undershoot value of MOOA-PID is 0.889% better than MOOA-PI. Detailed simulation results from the third case study can be seen in Table IX.

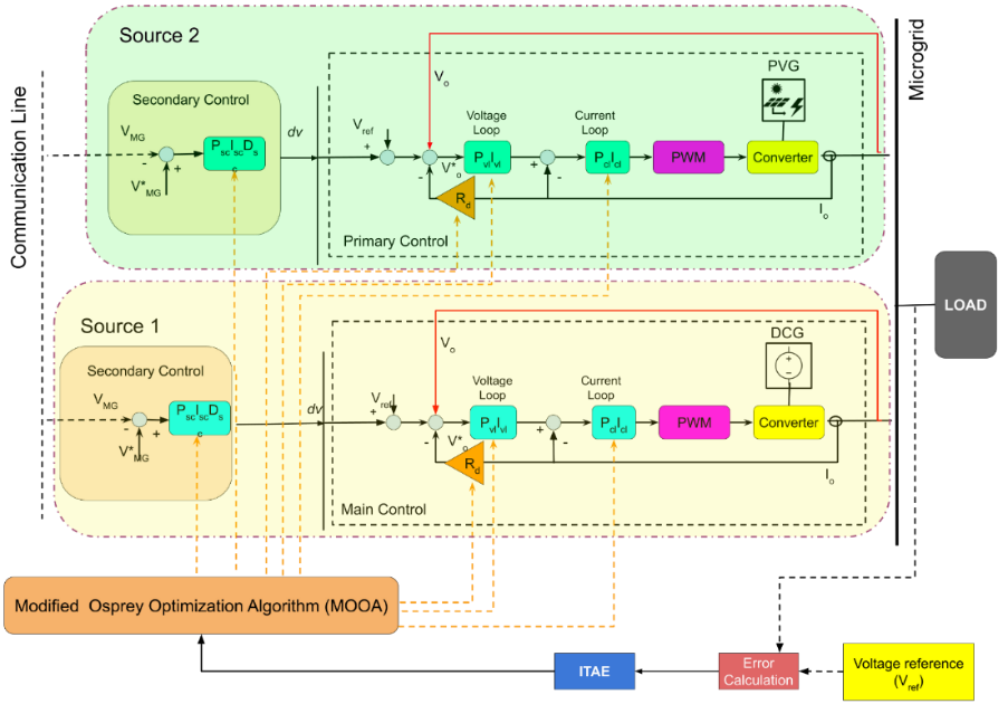

Fig. 6. Simple structure of DC microgrid with proposed method

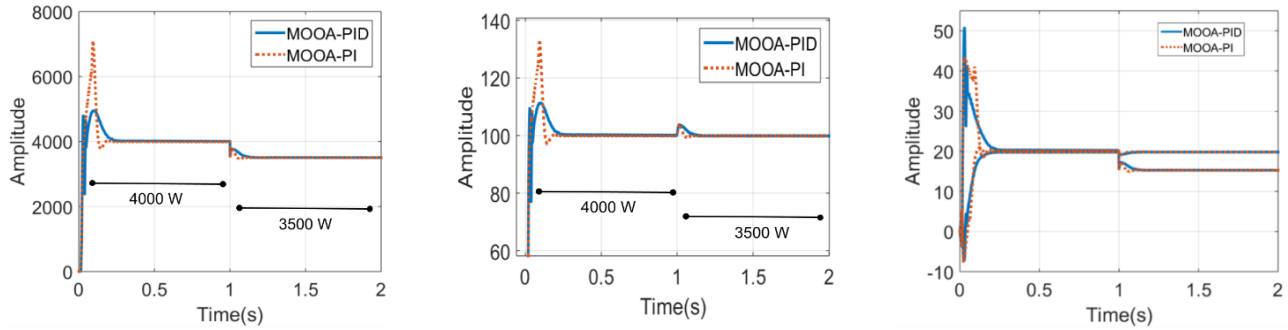

(a) (b) (c)

Fig. 7. System response from case 1 to (a) Power (b) Voltage (c) Current

TABLE V. EACH ALGORITHM'S VALUE OF CONTROL IN SOURCE 1

Methods	P_{vl}	I_{vl}	P_{cl}	I_{cl}	P_{sc}	I_{sc}	D_{sc}	R_{dcm}
No Secondary Control	0.6723	0.2379	0.1824	0.6808				0.8977
MOOA-PI	0.0639	0.9086	0.1412	0.7307	0.0271	136		0.8977
MOOA-PID	0.0639	0.9086	0.1412	0.7307	0.1756	29.59	0.0032	0.8977

TABLE VI. EACH ALGORITHM'S VALUE OF CONTROL IN SOURCE 2

Methods	P_{vl}	I_{vl}	P_{cl}	I_{cl}	P_{sc}	I_{sc}	D_{sc}	R_{dcm}
No Secondary Control	0.8368	0.6668	0.3202	0.2897				0.2200
MOOA-PI	0.5865	0.4116	0.3948	0.5807	0.0274	191		0.2200
MOOA-PID	0.5865	0.4116	0.3948	0.5807	0.1934	83.09	0.0185	0.2200

TABLE VII. TRANSIENT RESPONSE OF VOLTAGE IN CASE 1

	Time (0 -1) Seconds		Time (1 -2) Seconds		ITAE	ITSE
Methods	Overshoot	Undershoot	Overshoot	Undershoot		
MOOA-PI	132.4	93.34	103.9	99.47	0.7367	0.2249
MOOA-PID	110.1	99.39	103.7	99.89	0.7931	0.1323

TABLE VIII. TRANSIENT RESPONSE OF VOLTAGE IN CASE 2

	Time (0 -1) Seconds		Time (1 -2) Seconds		ITAE	ITSE
Methods	Overshoot	Undershoot	Overshoot	Undershoot		
MOOA-PI	139.1	88.82	100.8	92	0.6016	0.6093
MOOA-PID	119.7	99.14	100.4	93.86	0.6726	0.5012

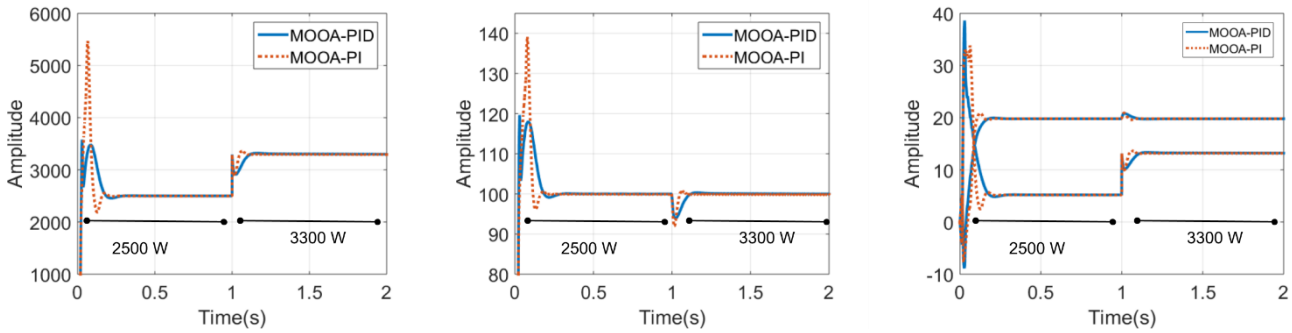

(a) (b) (c)

Fig. 8. System response from case 2 to (a) Power (b) Voltage (c) Current

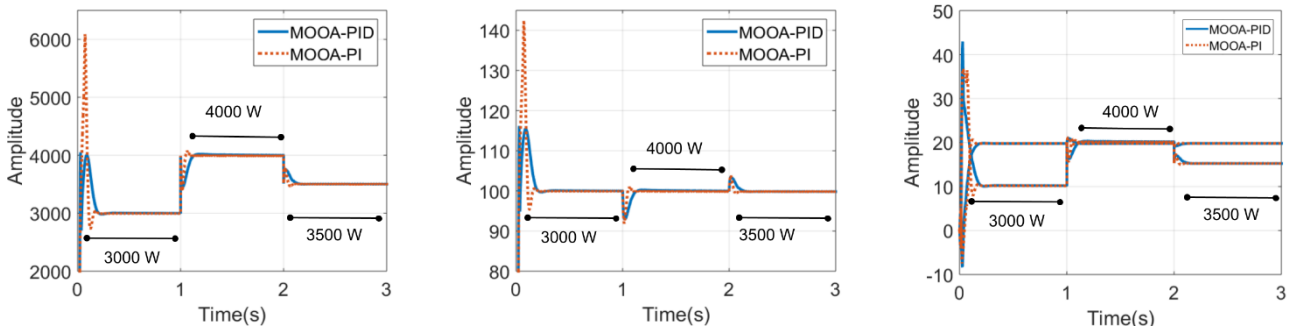

(a) (b) (c)

Fig. 9. System response from case 3 to (a) Power (b) Voltage (c) Current

TABLE IX. TRANSIENT RESPONSE OF VOLTAGE IN CASE 3

	Time (0 -1) Seconds		Time (1 -2) Seconds		Time (2 -3) Seconds		ITAE	ITSE
Methods	**Overshoot**	**Undershoot**	**Overshoot**	**Undershoot**	**Overshoot**	**Undershoot**		
MOOA-PI	142.5	95.37	100.9	91.9	103.9	99.38	0.6016	0.6093
MOOA-PID	116.2	94.89	100.4	92.86	103.5	99.89	0.6726	0.5012

V. CONCLUSION

The Osprey Optimization Algorithm (OOA) is a method that imitates the life of ospreys in nature. Levy flight is a phenomenon that occurs in random movements in nature, where the movement steps taken follow a levy distribution. Levy flights can be more efficient than other random movement patterns due to the possibility of taking large strides that potentially cover distant and unexplored territories. This research presents a modified OOA method by adding the Lévy flight method. The proposed method is named Modified Osprey Optimization Algorithm (MOOA). Apart from that, this research also describes the application of Proportional Integral Derivative (PID) control to MOOA-based secondary control. The MOOA method is applied to optimize the PID. Validation of this research uses 2 case studies. The first case study compares MOOA with One-to-One Based Optimizer (OOBO), Preschool Educational Optimization Algorithm (PEOA), and red-tailed hawk (RTH) algorithm using the CEC2017 benchmark function. The second case study compared the application of the MOOA method to PID and PI to secondary controls. From the simulation carried out in the first case study of the application of aviation levies to OOA, better exploration and exploitation results were obtained. MOOA has better results on 20 of 23 CEC2017 benchmark functions than OOA. MOOA can conduct exploration and exploitation faster and deeper to achieve convergent value. In the second case study, the implementation of PID with MOOA shows promising performance. The average voltage overshoot value from MOOA-PID is 9.828% better than MOOA-PI and the average voltage undershoot value from MOOA-PID is 2.887% better than MOOA-PI.

In future work, it would be interesting to apply the proposed MOOA algorithm to different and more complex datasets. MOOA has better exploration and exploitation which has the potential to be applied in solving optimization problems such as DC motor control, PV parameters, etc. Apart from that, it is necessary to study the application with other algorithms. Meanwhile, droop control needs to be explored more deeply in the application of the latest control methods.

REFERENCES

[1] A. Menati, K. Lee, and L. Xie, "Modeling and analysis of utilizing cryptocurrency mining for demand flexibility in electric energy systems: A synthetic texas grid case study," *IEEE Trans. Energy Mark. Policy Regul.*, vol. 1, no. 1, pp. 1–10, 2023.

[2] A. A. Ahmed, A. Alsharif, and N. Yasser, "Recent advances in energy storage technologies," *Int. J. Electr. Eng. Sustain.*, pp. 9–17, 2023.

[3] M. Wen, C. Zhou, and M. Konstantin, "Deep neural network for predicting changing market demands in the energy sector for a sustainable economy," *Energies*, vol. 16, no. 5, p. 2407, 2023.

[4] F. S. Al-Ismail, M. S. Alam, M. Shafiullah, M. I. Hossain, and S. M. Rahman, "Impacts of Renewable Energy Generation on Greenhouse Gas Emissions in Saudi Arabia: A Comprehensive Review," *Sustainability*, vol. 15, no. 6, p. 5069, 2023.

[5] F. L. Fuga and D. S. Ramos, "Proposals to improve the demand response in Brazil," *Electr. J.*, vol. 36, no. 1, p. 107237, 2023.

[6] T. Tröndle, J. Lilliestam, S. Marelli, and S. Pfenninger, "Trade-offs between geographic scale, cost, and infrastructure requirements for fully renewable electricity in Europe," *Joule*, vol. 4, no. 9, pp. 1929–1948, 2020.

[7] F. Taghizadeh-Hesary, E. Rasoulinezhad, M. Shahbaz, and X. V. Vo, "How energy transition and power consumption are related in Asian economies with different income levels?," *Energy*, vol. 237, p. 121595, 2021.

[8] L. Melnyk, H. Sommer, O. Kubatko, M. Rabe, and S. Fedyna, "The economic and social drivers of renewable energy development in OECD countries," *Probl. Perspect. Manag.*, vol. 18, no. 4, p. 37, 2021.

[9] M. Kumar, "Social, economic, and environmental impacts of renewable energy resources," *Wind Sol. hybrid Renew. energy Syst.*, vol. 1, 2020.

[10] N. Bamati and A. Raoofi, "Development level and the impact of technological factor on renewable energy production," *Renew. Energy*, vol. 151, pp. 946–955, 2020.

[11] Y. Bai *et al.*, "Flexibility quantification and enhancement of flexible electric energy systems in buildings," *J. Build. Eng.*, vol. 68, p. 106114, 2023.

[12] M. S. Bakare, A. Abdulkarim, M. Zeeshan, and A. N. Shuaibu, "A comprehensive overview on demand side energy management towards smart grids: challenges, solutions, and future direction," *Energy Informatics*, vol. 6, no. 1, pp. 1–59, 2023.

[13] A. Chadly, R. R. Urs, M. Wei, M. Maalouf, and A. Mayyas, "Techno-economic assessment of energy storage systems in green buildings while considering demand uncertainty," *Energy Build.*, vol. 291, p. 113130, 2023.

[14] G. E. Halkos and A. S. Tsirivis, "Electricity production and sustainable development: The role of renewable energy sources and specific socioeconomic factors," *Energies*, vol. 16, no. 2, p. 721, 2023.

[15] A. Raihan, M. Rashid, L. C. Voumik, S. Akter, and M. A. Esquivias, "The dynamic impacts of economic growth, financial globalization, fossil fuel, renewable energy, and urbanization on load capacity factor in Mexico," *Sustainability*, vol. 15, no. 18, p. 13462, 2023.

[16] M. Talaat, M. H. Elkholy, A. Alblawi, and T. Said, "Artificial intelligence applications for microgrids integration and management of hybrid renewable energy sources," *Artif. Intell. Rev.*, vol. 56, no. 9, pp. 10557-10611, 2023.

[17] R. Liu and Y. A. Solangi, "An Analysis of Renewable Energy Sources for Developing a Sustainable and Low-Carbon Hydrogen Economy in China," *Processes*, vol. 11, no. 4, p. 1225, 2023.

[18] A. Rafique, I. Ferreira, G. Abbas, and A. C. Baptista, "Recent advances and challenges toward application of fibers and textiles in integrated photovoltaic energy storage devices," *Nano-Micro Lett.*, vol. 15, no. 1, p. 40, 2023.

[19] C. Schubert *et al.*, "Hybrid Energy Storage Systems Based on Redox-Flow Batteries: Recent Developments, Challenges, and Future Perspectives," *Batteries*, vol. 9, no. 4, p. 211, 2023.

[20] Y. Sun *et al.*, "Surface chemistry and structure manipulation of graphene-related materials to address the challenges of electrochemical energy storage," *Chem. Commun.*, vol. 59, no. 18, pp. 2571–2583, 2023.

[21] M. Amir *et al.*, "Energy storage technologies: An integrated survey of developments, global economical/environmental effects, optimal scheduling model, and sustainable adaption policies," *J. Energy Storage*, vol. 72, p. 108694, 2023.

[22] S. Nahirniak, A. Ray, and B. Saruhan, "Challenges and future prospects of the MXene-based materials for energy storage applications," *Batteries*, vol. 9, no. 2, p. 126, 2023.

[23] Q. Hassan, A. Z. Sameen, H. M. Salman, M. Jaszczur, and A. K. Al-Jiboory, "Hydrogen energy future: Advancements in storage technologies and implications for sustainability," *J. Energy Storage*, vol. 72, p. 108404, 2023.

[24] M. Irfan, Y. Hao, M. Ikram, H. Wu, R. Akram, and A. Rauf, "Assessment of the public acceptance and utilization of renewable energy in Pakistan," *Sustain. Prod. Consum.*, vol. 27, pp. 312–324, 2021.

[25] W. Wang, B. Yuan, Q. Sun, and R. Wennersten, "Application of energy storage in integrated energy systems—A solution to fluctuation and uncertainty of renewable energy," *J. Energy Storage*, vol. 52, p. 104812, 2022.

[26] M. Abbasi, E. Abbasi, L. Li, R. P. Aguilera, D. Lu, and F. Wang, "Review on the microgrid concept, structures, components, communication systems, and control methods," *Energies*, vol. 16, no. 1, p. 484, 2023.

[27] M. Uddin, H. Mo, D. Dong, S. Elsawah, J. Zhu, and J. M. Guerrero, "Microgrids: A review, outstanding issues and future trends," *Energy Strateg. Rev.*, vol. 49, p. 101127, 2023.

[28] A. Micallef, J. M. Guerrero, and J. C. Vasquez, "New Horizons for Microgrids: From Rural Electrification to Space Applications," *Energies*, vol. 16, no. 4, p. 1966, 2023.

[29] C. -C. Liu *et al.*, "Microgrid Building Blocks: Concept and Feasibility," in *IEEE Open Access Journal of Power and Energy*, vol. 10, pp. 463-476, 2023.

[30] L. Zhou, Q. Liu, Y. Chen, Q. Ning, Z. Xiao and S. Wang, "Digital-Power-Communication Concept for Energy Coordination in PV-Battery-Charging DC Microgrid," in *IEEE Transactions on Smart Grid*, vol. 14, no. 6, pp. 4219-4229, Nov. 2023.

[31] A. Saleh *et al.*, "Optimal model predictive control for virtual inertia control of autonomous microgrids," *Sustainability*, vol. 15, no. 6, p. 5009, 2023.

[32] V. Khare and P. Chaturvedi, "Design, control, reliability, economic and energy management of microgrid: A review," *e-Prime-Advances Electr. Eng. Electron. Energy*, p. 100239, 2023.

[33] R. Förster, M. Kaiser, and S. Wenninger, "Future vehicle energy supply-sustainable design and operation of hybrid hydrogen and electric microgrids," *Appl. Energy*, vol. 334, p. 120653, 2023.

[34] F. Y. Vincent, T. H. A. Le, and J. N. D. Gupta, "Sustainable microgrid design with peer-to-peer energy trading involving government subsidies and uncertainties," *Renew. Energy*, vol. 206, pp. 658–675, 2023.

[35] L. M. León, D. Romero-Quete, N. Merchán, and C. A. Cortés, "Optimal design of PV and hybrid storage based microgrids for healthcare and government facilities connected to highly intermittent utility grids," *Appl. Energy*, vol. 335, p. 120709, 2023.

[36] I. Ahmed, A. Basit, F. e Mustafa, M. Alqahtani, and M. Khalid, "The nexus of energy in microgrids: A review on communication barriers in distributed networks auxiliary controls," *IET Gener. Transm. Distrib.*, vol. 17, no. 22, pp. 4907-4922, 2023.

[37] Y. Huang *et al.*, "Multi-objective optimization of campus microgrid system considering electric vehicle charging load integrated to power grid," *Sustain. Cities Soc.*, vol. 98, p. 104778, 2023.

[38] A. Albaker, M. Alturki, R. Abbassi, and K. Alqunun, "Zonal-Based Optimal Microgrids Identification," *Energies*, vol. 15, no. 7, p. 2446, 2022.

[39] M. Debouza, A. Al-Durra, T. H. M. EL-Fouly, and H. H. Zeineldin, "Survey on microgrids with flexible boundaries: Strategies, applications, and future trends," *Electr. Power Syst. Res.*, vol. 205, p. 107765, 2022.

[40] M. Mathew, M. S. Hossain, S. Saha, S. Mondal, and M. E. Haque, "Sizing approaches for solar photovoltaic-based microgrids: A comprehensive review," *IET Energy Syst. Integr.*, vol. 4, no. 1, pp. 1–27, 2022.

[41] S. Kumar, R. Sharma, S. S. Murthy, P. Dutta, W. He, and J. Wang, "Thermal analysis and optimization of stand-alone microgrids with metal hydride based hydrogen storage," *Sustain. Energy Technol. Assessments*, vol. 52, p. 102043, 2022.

[42] K. Shankar, S. R. Salkuti, and S.-C. Kim, "Review on Microgrids: Types, Challenges, Opportunities, Uncertainties, and Their Modeling," *Power Qual. Microgrids Issues, Challenges Mitig. Tech.*, pp. 363–389, 2023.

[43] B. Modu, M. P. Abdullah, M. A. Sanusi, and M. F. Hamza, "DC-Based microgrid: Topologies, control schemes, and implementations," *Alexandria Eng. J.*, vol. 70, pp. 61–92, 2023.

[44] M. A. Ahmed, G. Abbas, T. A. Jumani, N. Rashid, A. A. Bhutto, and S. M. Eldin, "Techno-economic optimal planning of an industrial microgrid considering integrated energy resources," *Front. Energy Res.*, vol. 11, p. 1145888, 2023.

[45] Z.-L. Li, P. Li, Z.-P. Yuan, J. Xia, and D. Tian, "Optimized utilization of distributed renewable energies for island microgrid clusters considering solar-wind correlation," *Electr. Power Syst. Res.*, vol. 206, p. 107822, 2022.

[46] A. H. Tariq, S. A. A. Kazmi, M. Hassan, S. A. M. Ali, and M. Anwar, "Analysis of fuel cell integration with hybrid microgrid systems for clean energy: A comparative review," *Int. J. Hydrogen Energy*, vol. 52, pp. 1005-1034, 2023.

[47] N. T. Mbungu, A. A. Ismail, M. AlShabi, R. C. Bansal, A. Elnady, and A. K. Hamid, "Control and estimation techniques applied to smart microgrids: A review," *Renew. Sustain. Energy Rev.*, vol. 179, p. 113251, 2023.

[48] M. Ehjaz, M. IQBAL, S. S. H. ZAİDİ, and K. Bilal, "Design and implementation of a peer-to-peer energy trading scheme in multi-microgrid network with photovoltaics and wind energy," *J. Energy Syst.*, vol. 7, no. 2, pp. 158–172, 2023.

[49] M. Daisy, M. H. Aliabadi, S. Javadi, and H. M. Naimi, "A robust transient and sustainable faults location approach for AC microgrid based on voltage and current difference measurements," *Int. J. Electr. Power Energy Syst.*, vol. 153, p. 109343, 2023.

[50] D. Jain and D. Saxena, "Comprehensive review on control schemes and stability investigation of hybrid AC-DC microgrid," *Electr. Power Syst. Res.*, vol. 218, p. 109182, 2023.

[51] S. A. Hosseini, B. Taheri, S. H. H. Sadeghi, and A. Nasiri, "An Overview of DC Microgrid Protection Schemes and the Factors Involved," *Electr. Power Components Syst.*, pp. 1–31, 2023.

[52] B. Sahoo, S. K. Routray, and P. K. Rout, "AC, DC, and hybrid control strategies for smart microgrid application: A review," *Int. Trans. Electr. Energy Syst.*, vol. 31, no. 1, p. e12683, 2021.

[53] O. Azeem *et al.*, "A comprehensive review on integration challenges, optimization techniques and control strategies of hybrid AC/DC Microgrid," *Appl. Sci.*, vol. 11, no. 14, p. 6242, 2021.

[54] J. Singh, S. Prakash Singh, K. Shanker Verma, A. Iqbal, and B. Kumar, "Recent control techniques and management of AC microgrids: A critical review on issues, strategies, and future trends," *Int. Trans. Electr. Energy Syst.*, vol. 31, no. 11, p. e13035, 2021.

[55] F. S. Al-Ismail, "DC Microgrid Planning, Operation, and Control: A Comprehensive Review," in *IEEE Access*, vol. 9, pp. 36154-36172, 2021.

[56] V. F. Pires, A. Pires, and A. Cordeiro, "DC Microgrids: Benefits, Architectures, Perspectives and Challenges," *Energies*, vol. 16, no. 3, p. 1217, 2023.

[57] S. S. Rangarajan *et al.*, "DC microgrids: a propitious smart grid paradigm for smart cities," *Smart Cities*, vol. 6, no. 4, pp. 1690–1718, 2023.

[58] A.-C. Braitor, G. C. Konstantopoulos, and V. Kadirkamanathan, "Current-limiting droop control design and stability analysis for paralleled boost converters in DC microgrids," *IEEE Trans. Control Syst. Technol.*, vol. 29, no. 1, pp. 385–394, 2020.

[59] Y. C. C. Wong, C. S. Lim, M. D. Rotaru, A. Cruden, and X. Kong, "Consensus virtual output impedance control based on the novel droop equivalent impedance concept for a multi-bus radial microgrid," *IEEE Trans. Energy Convers.*, vol. 35, no. 2, pp. 1078–1087, 2020.

[60] X. He, V. Häberle, I. Subotić, and F. Dörfler, "Nonlinear Stability of Complex Droop Control in Converter-Based Power Systems," *IEEE Control Syst. Lett.*, vol. 7, pp. 1327–1332, 2023.

[61] P. Sun, Y. Wang, M. Khalid, R. Blasco-Gimenez, and G. Konstantinou, "Steady-state power distribution in VSC-based MTDC systems and dc grids under mixed P/V and I/V droop control," *Electr. Power Syst. Res.*, vol. 214, p. 108798, 2023.

[62] N. A. Sevostyanov and R. L. Gorbunov, "Control Strategy to Mitigate Voltage Ripples in Droop-Controlled DC Microgrids," in *IEEE Transactions on Power Electronics*, vol. 38, no. 12, pp. 15377-15389, Dec. 2023.

[63] S. Liu, H. Miao, J. Li, and L. Yang, "Voltage control and power sharing in DC Microgrids based on voltage-shifting and droop slope-adjusting strategy," *Electr. Power Syst. Res.*, vol. 214, p. 108814, 2023.

[64] M. Carnaghi, P. Cervellini, M. Judewicz, R. G. Retegui, and M. Funes, "Stability analysis of a Networking DC microgrid with distributed droop control and CPLs," *IEEE Lat. Am. Trans.*, vol. 21, no. 9, pp. 966–975, 2023.

[65] O. Ja'afreh, J. Siam, and H. Shehadeh, "Power Loss and Total Load Demand Coverage in Stand-Alone Microgrids: A Combined and Conventional Droop Control Perspectives," *IEEE Access*, vol. 10, pp. 128721–128731, 2022.

[66] N. Bhatt, R. Sondhi, and S. Arora, "Droop control strategies for microgrid: A review," *Adv. Renew. Energy Electr. Veh. Sel. Proc. AREEV 2020*, pp. 149–162, 2022.

[67] F. Lu and H. Liu, "An Accurate Power Flow Method for Microgrids with Conventional Droop Control," *Energies*, vol. 15, no. 16, p. 5841, 2022.

[68] G. Lin, W. Zuo, Y. Li, J. Liu, S. Wang, and P. Wang, "Comparative analysis on the stability mechanism of droop control and VID control in DC microgrid," *Chinese J. Electr. Eng.*, vol. 7, no. 1, pp. 37–46, 2021.

[69] Y. Zhang, X. Qu, M. Tang, R. Yao, and W. Chen, "Design of nonlinear droop control in DC microgrid for desired voltage regulation and current sharing accuracy," *IEEE J. Emerg. Sel. Top. Circuits Syst.*, vol. 11, no. 1, pp. 168–175, 2021.

[70] Y. Han, X. Ning, L. Li, P. Yang, and F. Blaabjerg, "Droop coefficient correction control for power sharing and voltage restoration in hierarchical controlled DC microgrids," *Int. J. Electr. Power Energy Syst.*, vol. 133, p. 107277, 2021.

[71] R. Kumar and M. K. Pathak, "Distributed droop control of dc microgrid for improved voltage regulation and current sharing," *IET Renew. Power Gener.*, vol. 14, no. 13, pp. 2499-2506 2020.

[72] Shivam and R. Dahiya, "Distributed control for DC microgrid based on optimized droop parameters," *IETE J. Res.*, vol. 66, no. 2, pp. 192–203, 2020.

[73] Z. Li, K. W. Chan, J. Hu, and J. M. Guerrero, "Adaptive droop control using adaptive virtual impedance for microgrids with variable PV outputs and load demands," *IEEE Trans. Ind. Electron.*, vol. 68, no. 10, pp. 9630–9640, 2020.

[74] D. Baros, N. Rigogiannis, N. Papanikolaou, and M. Loupis, "Investigation of communication delay impact on DC microgrids with adaptive droop control," in *2020 International Symposium on Industrial Electronics and Applications (INDEL)*, pp. 1–6, 2020.

[75] Y. Xiong *et al.*, "Adaptive dual droop control of MTDC integrated offshore wind farms for fast frequency support," *IEEE Trans. Power Syst.*, vol. 38, no. 3, pp. 2525–2538, 2022.

[76] Y. Shen, W. Wu, B. Wang, and S. Sun, "Optimal Allocation of Virtual Inertia and Droop Control for Renewable Energy in Stochastic Look-Ahead Power Dispatch," in *IEEE Transactions on Sustainable Energy*, vol. 14, no. 3, pp. 1881-1894, July 2023.

[77] A. H. Lone and N. Gupta, "A novel load flow method for islanded microgrids with optimum droop coefficients," *e-Prime-Advances Electr. Eng. Electron. Energy*, vol. 6, p. 100341, 2023.

[78] C. Guo, J. Liao, and Y. Zhang, "Adaptive droop control of unbalanced voltage in the multi-node bipolar DC microgrid based on fuzzy control," *Int. J. Electr. Power Energy Syst.*, vol. 142, p. 108300, 2022.

[79] A. Yavuz, N. Celik, C.-H. Chen, and J. Xu, "A Sequential Sampling-based Particle Swarm Optimization to Control Droop Coefficients of Distributed Generation Units in Microgrid Clusters," *Electr. power Syst. Res.*, vol. 216, p. 109074, 2023.

[80] H. Zhang, S. Gao, and P. Zhou, "Role of digitalization in energy storage technological innovation: Evidence from China," *Renew. Sustain. Energy Rev.*, vol. 171, p. 113014, 2023.

[81] X. Xianyong and Z. Zixuan, "New Power Systems Dominated by Renewable Energy Towards the Goal of Emission Peak & Carbon Neutrality: Contribution, Key Techniques, and Challenges.," *Adv. Eng. Sci. Kexue Yu Jishu*, vol. 54, no. 1, 2022.

[82] M. Dehghani, E. Trojovská, P. Trojovský, and O. P. Malik, "OOBO: A New Metaheuristic Algorithm for Solving Optimization Problems,"

Biomimetics, vol. 8, no. 6, p. 468, 2023.

[83] P. Trojovský, "A new human-based metaheuristic algorithm for solving optimization problems based on preschool education," *Sci. Rep.*, vol. 13, no. 1, p. 21472, 2023.

[84] S. Ferahtia *et al.*, "Red-tailed hawk algorithm for numerical optimization and real-world problems," *Sci. Rep.*, vol. 13, no. 1, p. 12950, 2023.

[85] L. Zhang, H. Zheng, Q. Hu, B. Su, and L. Lyu, "An adaptive droop control strategy for islanded microgrid based on improved particle swarm optimization," *IEEE Access*, vol. 8, pp. 3579–3593, 2019.

[86] R. P. Nair and P. Kanakasabapathy, "PR controller-based droop control strategy for AC microgrid using Ant Lion Optimization technique," *Energy Reports*, vol. 9, pp. 6189–6198, 2023.

[87] T. A. Jumani, M. Mustafa, W. Anjum, and S. Ayub, "Salp swarm optimization algorithm-based controller for dynamic response and power quality enhancement of an islanded microgrid," *Processes*, vol. 7, no. 11, p. 840, 2019.

[88] J. Kumar, A. Agarwal, and V. Agarwal, "A review on overall control of DC microgrids," *J. energy storage*, vol. 21, pp. 113–138, 2019.

[89] F. Gao, R. Kang, J. Cao, and T. Yang, "Primary and secondary control in DC microgrids: a review," *J. Mod. Power Syst. Clean Energy*, vol. 7, no. 2, pp. 227–242, 2019.

[90] S. Ansari, A. Chandel, and M. Tariq, "A comprehensive review on power converters control and control strategies of AC/DC microgrid," *IEEE Access*, vol. 9, pp. 17998–18015, 2020.

[91] N. Ghanbari and S. Bhattacharya, "Adaptive droop control method for suppressing circulating currents in dc microgrids," *IEEE Open Access J. Power Energy*, vol. 7, pp. 100–110, 2020.

[92] G. Wang, G. Duan, J. Duan, S. Cao, Y. Song, and J. Kang, "An integrated control method of multi-source Islanded microgrids," *Energy Reports*, vol. 9, pp. 630–636, 2023.

[93] N. Khosravi *et al.*, "A novel control approach to improve the stability of hybrid AC/DC microgrids," *Appl. Energy*, vol. 344, p. 121261, 2023.

[94] D. N. Nguyen and T. A. Nguyen, "Proposing an original control algorithm for the active suspension system to improve vehicle vibration: Adaptive fuzzy sliding mode proportional-integral-derivative tuned by the fuzzy (AFSPIDF)," *Heliyon*, vol. 9, no. 3, 2023.

[95] N. M. Dawoud, T. F. Megahed, and S. S. Kaddah, "Enhancing the performance of multi-microgrid with high penetration of renewable energy using modified droop control," *Electr. Power Syst. Res.*, vol. 201, p. 107538, 2021.

[96] N. B. Roy and D. Das, "Probabilistic optimal power dispatch in a droop controlled islanded microgrid in presence of renewable energy sources and PHEV load demand," *Renew. Energy Focus*, vol. 45, pp. 93–122, 2023.

[97] P. Lusis, L. L. H. Andrew, A. Liebman, and G. Tack, "Interaction between coordinated and droop control PV inverters," in *Proceedings of the Eleventh ACM International Conference on Future Energy Systems*, pp. 314–324, 2020.

[98] R. Xu, C. Zhang, Y. Xu, Z. Dong, and R. Zhang, "Multi-objective hierarchically-coordinated volt/var control for active distribution networks with droop-controlled PV inverters," *IEEE Trans. Smart Grid*, vol. 13, no. 2, pp. 998–1011, 2021.

[99] R. El-Sehiemy, A. Shaheen, A. Ginidi, and S. F. Al-Gahtani, "Proportional-Integral-Derivative Controller Based-Artificial Rabbits Algorithm for Load Frequency Control in Multi-Area Power Systems," *Fractal Fract.*, vol. 7, no. 1, p. 97, 2023.

[100] M. Dehghani and P. Trojovský, "Osprey optimization algorithm: A new bio-inspired metaheuristic algorithm for solving engineering optimization problems," *Frontiers in Mechanical Engineering* , vol. 8. 2023.

[101] P. Barthelemy, J. Bertolotti, and D. S. Wiersma, "A Lévy flight for light," *Nature*, vol. 453, no. 7194, pp. 495-498, 2008.

[102] R. N. Mantegna, "Fast, accurate algorithm for numerical simulation of Lévy stable stochastic processes," *Phys. Rev. E*, vol. 49, no. 5, p. 4677, 1994.